

Dehydration melting of crustal rocks

ALAN BRUCE THOMPSON

Departement für Erdwissenschaften Eidgenössische Technische Hochschule Zürich CH-8092 Zürich, Switzerland

Introduction

It has been long known from experimental studies (eg. TUTTLE and BOWEN, 1958; WINKLER, 1979) that excess H_2O greatly depresses the solidus temperature of crustal rocks, and also that the amount of water needed to saturate such anatectic melts is considerable. LUTH (1976; Table 1), in summarising the data of previous workers, notes that at 10 bar PH_2O the solidus temperature is as low as 620°C for the «granite minimum» (in the system $NaAlSi_3O_8$ (Ab) + $KAlSi_3O_8$ (Or) + SiO_2 (Qz) + H_2O) and has a composition (wt%) of (Ab) 46.15: (Or) 17.5: (Qz) 19: (H_2O) 17. This amount of H_2O is far in excess of that available in common hydrated minerals (Muscovite (Mus) ~ 4.5 wt%; Biotite (Bio) ~ 4.3 wt%; Amphibole (Amp) ~ 2-1.5 wt%). Thus for water-saturated melting to occur, either enormous volumes of metamorphic rocks need to dehydrate conveniently close to where feldspar + quartz rocks are waiting to be melted at depth in the crust, or that the amounts of melt produced from the release of H_2O from hydrated minerals is really quite small at temperatures just above the region of the H_2O -saturated solidus.

The amount of anatectic melt generated from any rock composition (in addition to its composition and physical properties) will determine its ability to separate from its restite, segregate into melt pools and ascend. In addition to temperature and the amount

of water available at the melting site, the quantity of melt generated depends primarily upon how closely the proportions of quartz, alkali-feldspar and plagioclase in the rock approach the «granite minimum» composition for any particular pressure and aH_2O . If free water is not available then the amount of melt is proportional to the amount of hydrous minerals present. Thus most crustal rock types

TABLE 1

H₂O contents of Ab + Or + Qz liquids close to the H₂O-saturated solidus, calculated from the data summarised by LUTH (1976, Table 1) according to the method of BURNHAM (1979a, and b)

P(bar)	T(°C)	weight percent			mole percent		
		Ab	Or	Qz	H ₂ O	H ₂ O	*
1	990						
490	770	29	29	39	3.0	30.6	
980	720	31.5	27.7	36.3	4.4	39.7	
1961	685	36.5	24.3	32.7	6.5	49.9	
2942	665	38.5	30	30.2	8.3	54.8	
4000	655	42.3	20.7	27	9.9	61.2	
5000	640	44.5	19.6	24.9	11.0	64.0	
10000	620	46.5	17.5	19	17.0	78.4	

* using molecular weight Ab = 262,225; Or = 278,337; Si_4O_8 = 240,34; H_2O = 18,015.

will undergo vapour-absent melting as mica or amphibole dehydrate and simultaneously melt to produce H_2O -undersaturated «granitic» liquids. Melting will therefore proceed in a series of steps as the hydrous minerals undergo successive dehydration-

melting. It is therefore appropriate to consider first the nature of dehydration-melting of muscovite, biotite and amphibole in simple systems, then in model or real rocks, at various depths in the crust. In addition it is necessary to consider the nature of the heat sources responsible for the endothermic melting reactions and their duration, as well as considering the scale and duration of fluid movement (especially H_2O) in the lower crust and in the anatectic liquids themselves.

The approach used is deliberately simplified both thermodynamically in calculations and graphically in illustrations. As emphasised by the philosophy of the meeting in Siena, one purpose is to provide a framework by which important questions can be partly answered by the available data and simplified theoretical concepts. I apologise to colleagues who rightly expect sometimes a more rigorous approach and I have attempted, where possible, to indicate where more thorough discussions are available, or need to be.

Some generalisations about the compositions of crustal anatectic melts

The anatectic behaviour of most crustal rocks types is relatable to the experimentally known melting reactions of quartz-feldspar mixtures. Experimental studies (Fig. 1) in the «granite» system ($Ab + Or + Qz + H_2O$) have shown that with increasing pressure at H_2O -saturation the minimum becomes eutectic (Fig. 1) and moves away from Qz towards Ab , whereas when dry, the minimum/eutectic moves away from Qz towards Or (see summary diagrams by WYLLIE, 1977; Fig. 1). The role of plagioclase melting through the incorporation of the $CaAl_2Si_2O_8$ (*an*) component is also reasonably well understood with increasing pressure, especially at H_2O -saturation (see summaries by THOMPSON and TRACY, 1979; JOHANNES, 1985).

The most common rock types in the middle and lower crust are probably metabasalt (as amphibolite or mafic granulite/eclogite), quartzo-feldspathic rocks (referred to here as (preexisting) «granite» although including the whole range of felsic plutonics as well as metasediments) and metapelites. Carbonates

and ultramafics may be locally abundant but clearly their melting is not controlled by quartz-feldspar reactions. Preexisting granites have the optimum proportions of quartz and two feldspars to generate large amounts of «minimum» melt composition but will only do so at the temperatures of the H_2O -saturated solidus given the influx of large amounts of external water. The amounts of hydrous minerals in «granites» is much less than in metapelites. So «granites» have the optimum proportions of quartz and feldspar to produce more melt than metapelites with an excess of H_2O , but the latter contain more hydrous minerals for dehydration-melting.

Amphibolites rarely contain K-feldspar but often contain small amounts of quartz in contrast to their basalt source rock, mainly because many metamorphic minerals in amphibolites (eg. chlorite and amphibole) are low-silica minerals. So in amphibolites melting is initially controlled by plagioclase + quartz, then if the small amount of quartz is removed into the melt, plagioclase + amphibole melting would control subsequent anatexis. A consequence of quartz removal into early melts makes difficult many theoretical treatments of pelite or amphibolite melting which, because of graphical constraints, assume quartz saturation well into the melting interval. However, CLEMENS J.D. (pers. comm. April 1987) has suggested that for most quartzo-feldspathic rocks their ratio in controlling the amount of melt produced is probably only important for H_2O -saturated melting. Fluid-absent melting should not lead to near-solidus (early) exhaustion of either quartz or feldspar.

For most crustal rocks the melting temperature intervals are large, due mainly to the considerable divergence from the quartz-feldspar proportions of the «granite minimum» composition and the small amounts of H_2O available from dehydration melting compared to that required to saturate the melt (Figs. 2 and 3). Many minerals in metapelites and amphibolites are quite refractory and frequently persist to very high temperatures after quartz and feldspar disappearance, even at low water contents.

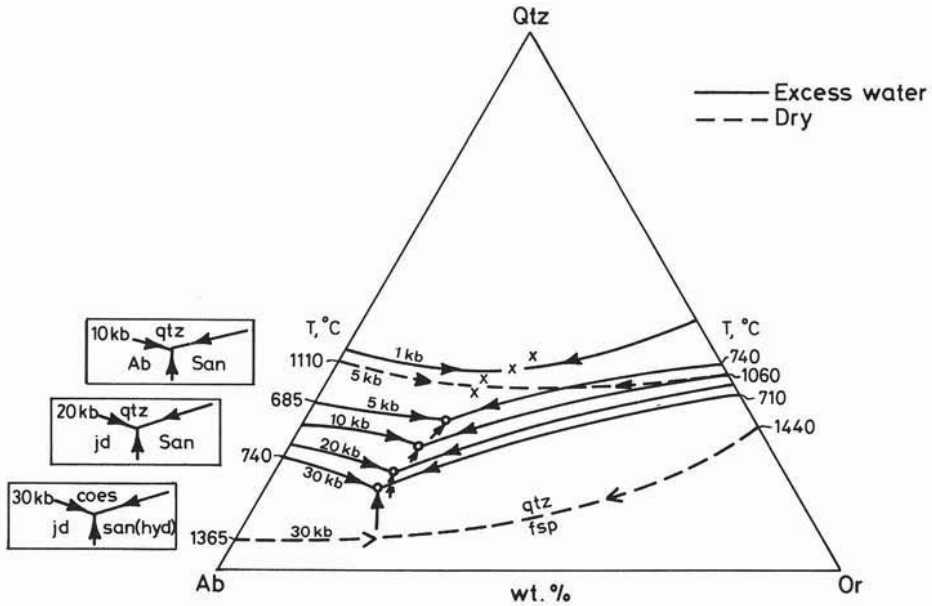


Fig. 1. — Effect of pressure on liquidus field boundaries in the systems Ab + Or + Qtz + H₂O (solid lines) and Ab + Or + Qtz (dashed lines), as summarised by WYLLIE (1977, Fig. 1, p. 44). Crosses and circles mark the compositions (wt%) of the minima/eutectica at various PH₂O (in kbar) and temperatures (°C). Abbreviations: qz (quartz), ab (albite), san (k-feldspar), jd (jadeite), coes (coesite), fsp (Na-K feldspar).

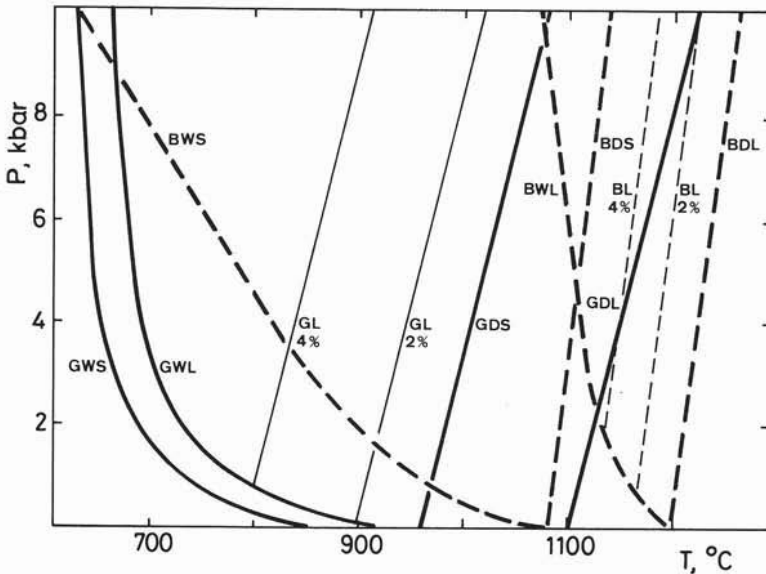


Fig. 2. — Pressure (kbar) - temperature (°C) diagram showing the anhydrous and H₂O-saturated solidus and liquidus curves for granite (heavy solid lines) as summarised by HARRIS et al. (1970, Fig. 1, p. 191). G = granite, B = basalt, W = H₂O-saturated, D = anhydrous, S = solidus, L = liquidus. Light lines show displacement of the liquidus with 2 and 4 wt% H₂O.

Moreover, the «granitic» melts can dissolve increasing amounts of non-quartz-feldspathic components (especially Al_2O_3 , FeO , MgO , CaO) with increasing temperature, as is discussed further below.

P-T-X(H_2O) relations in the granite system

From P-V-T (pressure-volume-temperature) measurements of partial molar volumes of melts in the system $\text{Ab} + \text{H}_2\text{O}$ (BURNHAM and DAVIS, 1971, 1974) and additional theoretical considerations, BURNHAM (1982) has developed a general model for P-T- aH_2O (water activity related to mole fraction, X_w^m of water in the melt) for granite-like melts. The general applicability of the model can be seen in Fig. 3a where BURNHAM's (1979; Fig. 16.6) data for the solubility surface in $\text{Ab} + \text{H}_2\text{O}$ (marked in the upper left inset diagram, Fig. 3b, by the H_2O -saturated melting-reaction $\text{V} + \text{Ab} = \text{L}$) has been extended to the granite system ($\text{Ab} + \text{Or} + \text{Qz} + \text{H}_2\text{O}$). To do this, the H_2O -solubility data in such melts (summarised by LUTH, 1978, p. 351, see also BURNHAM, 1982, Table 9.5) have been renormalised on the basis ($\text{NaAlSi}_3\text{O}_8 + \text{KAlSi}_3\text{O}_8 + \text{Si}_2\text{O}_8 + \text{H}_2\text{O}$) to convert wt% H_2O to mol% H_2O (Table 1). Both values (wt%, mol%, H_2O in the ($\text{Ab} + \text{Or} + \text{Qz} + \text{H}_2\text{O}$) melts) are shown next to the solid circles and the H_2O -saturated solidus for this system, where it can be seen that the renormalised values of X_w^m in ($\text{Ab} + \text{Or} + \text{Qz} + \text{H}_2\text{O}$) correspond well with the simple graphical extension of the H_2O -solubility saturation surface in $\text{Ab} + \text{H}_2\text{O}$. From these intersection points, the P-T-X(H_2O) surface for the H_2O -undersaturated region can be approximately contoured. Holloway (pers. comm. to JOHANNES, 1985, p. 41) has also calculated this surface using a much more rigorous approach and shows that dP/dT for X_w^m in ($\text{Ab} + \text{Or} + \text{Qz} + \text{H}_2\text{O}$) is slightly different from those for $\text{Ab} + \text{H}_2\text{O}$. In general support of the extrapolation of BURNHAM's (1982) melt model for granite like systems, it can be envisaged that experimentally measured solubility data for any feldspar + quartz + H_2O system (also in

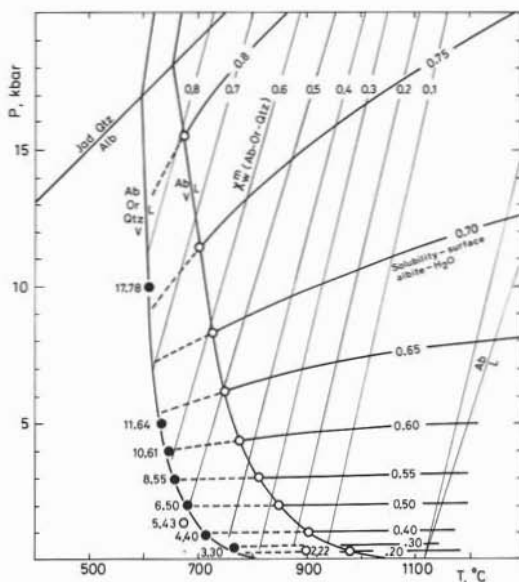


Fig. 3a. — Pressure-temperature projection of phase relations in the system $\text{NaAlSi}_3\text{O}_8 (\text{Ab}) + \text{H}_2\text{O} (\text{V})$ from BURNHAM (1979, Fig. 16.6), where the saturation (solubility) isopleths for the equilibrium ($\text{V} + \text{Ab} = \text{L}$) (Fig. 3b) have been extended to intersect the H_2O -saturated granite solidus ($\text{Ab} + \text{Or} + \text{Qz} + \text{V} = \text{L}$). The solid circles at the «granite-minimum» (Fig. 3a) show wt% H_2O in the melt and mol% (calculated on the basis of $\text{Ab} + \text{Or} + \text{Si}_2\text{O}_8 + \text{H}_2\text{O}$, from the data summarised by LUTH (1976)). The X_w^m isopleths, representing the amount of H_2O dissolved in H_2O -undersaturated «granite» melts, have been drawn using an ideal solution model, the H_2O values at saturation, and the slopes computed by HOLLOWAY J.R. (in JOHANNES, 1985).

the H_2O -deficient region) can be treated graphically (or better numerically through equations of state) in the same way. As has already been shown for several such investigations, the comparison of experiments with such simplified calculations provides refinement of the activity-composition relations in feldspar + quartz + H_2O system, also when the H_2O is diluted with species such as CO_2 , which may variously interact with melt components (especially An , $\text{CaAl}_2\text{Si}_2\text{O}_8$, see BURNHAM, 1979b, p. 77).

For the moment we will use the simplified version of the BURNHAM model as outlined above to estimate the X_w^m at any particular P and T relative to the H_2O -saturated and dry-melting (no free H_2O whatsoever) of the relevant quartz-feldspar systems. This means

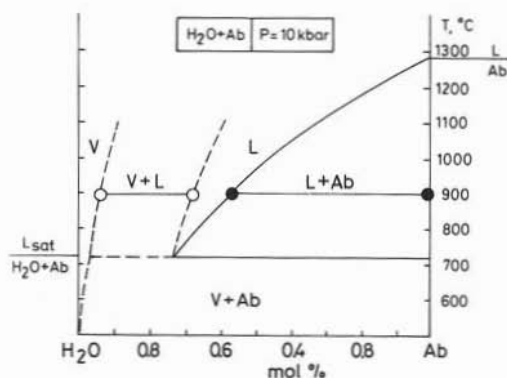


Fig. 3b. — A 10 kbar T-X section for Ab + H₂O, partly constructed from BURNHAM (1979a, Fig. 16.6) and the rest is schematic (dashed lines).

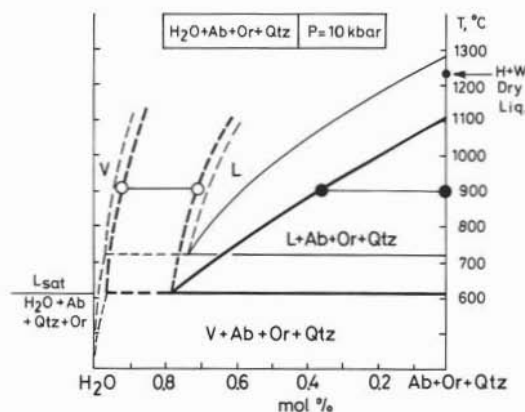


Fig. 3c. — A 10 kbar pseudo-binary T-X section for (Ab + Or + Qtz) + H₂O, constructed partly from Fig. 2 and Fig. 3a (solid lines) and the rest is schematic. Superimposed with lighter lines is the section from Fig. 3b. Schematic tie lines at 900°C show the relative H₂O contents of the phases. The dry liquidus from HUANG and WYLLIE (1981) is shown near 1240°C.

that the reference melting reactions can also change during progressive melting if either plagioclase, alkali-feldspar or quartz is initially absent from the subsolidus metamorphic rock, or is exhausted early by extraction into the melt (as discussed in section 2). By using X_m^w contours for the relevant feldspar (+ quartz + H₂O) compositions, modified when necessary to account for non-quartzofeldspathic components in the melt (see below), it is possible to calculate the amount of H₂O dissolved in any «granitic» melt at any P and T in the H₂O-undersaturated region. Then by allowing a specific amount

of H₂O to enter the melt, for example by the breakdown of muscovite, it is possible to estimate the amount of melt following the methods presented by BURNHAM (1967, 1979a) and CLEMENS (1984).

Dehydration-melting of mica in simplified systems

As examples of P-T-X(H₂O) relations of dehydration melting reactions, it is useful to consider a(H₂O)-X(H₂O) relations in the reference system $Or + Qtz + H_2O$, modified to account for the excess Al₂O₃ when muscovite, or excess MgO when phlogopite, undergoes dehydration melting. The P-T schematics of muscovite + quartz dehydration and melting reactions are shown in Fig. 4, with accompanying isobaric pseudo-binary T-X(rock-H₂O) diagrams at three arbitrary pressures. At pressures above the invariant point, muscovite rocks with excess water would melt at lower temperatures (through $H + V \rightarrow L$ in the pseudo-binary sections) than for rocks without water, where melting would occur incongruently through ($H \rightarrow L + A$). The abbreviations H for hydrous minerals and A for anhydrous assemblage used here, permit wider extrapolation of the concepts to biotite and amphibole systems. Important to note that at pressures below the invariant point (which occurs at about 5 kbar and 700°C according to LAMBERT et al., 1969, p. 622), that dehydration of Mus + Qtz occurs at temperatures below the H₂O-saturated solidus. In nature this dehydration water would need to remain at the production site to be (conveniently) available for H₂O-saturated melting during the progressive heating period between the two reactions. Because the amount of H₂O required to saturate granitic melts at low pressures is much less than at higher pressure (see Fig. 3a), even the amount of water from low-pressure breakdown of the biotite available in metapelites could produce sizeable melt proportions.

The dehydration melting of muscovite + quartz via:

$$\text{Mus} + \text{Qtz} \rightarrow \text{San} + \text{Als} + \text{H}_2\text{O-undersaturated melt} \quad (1)$$

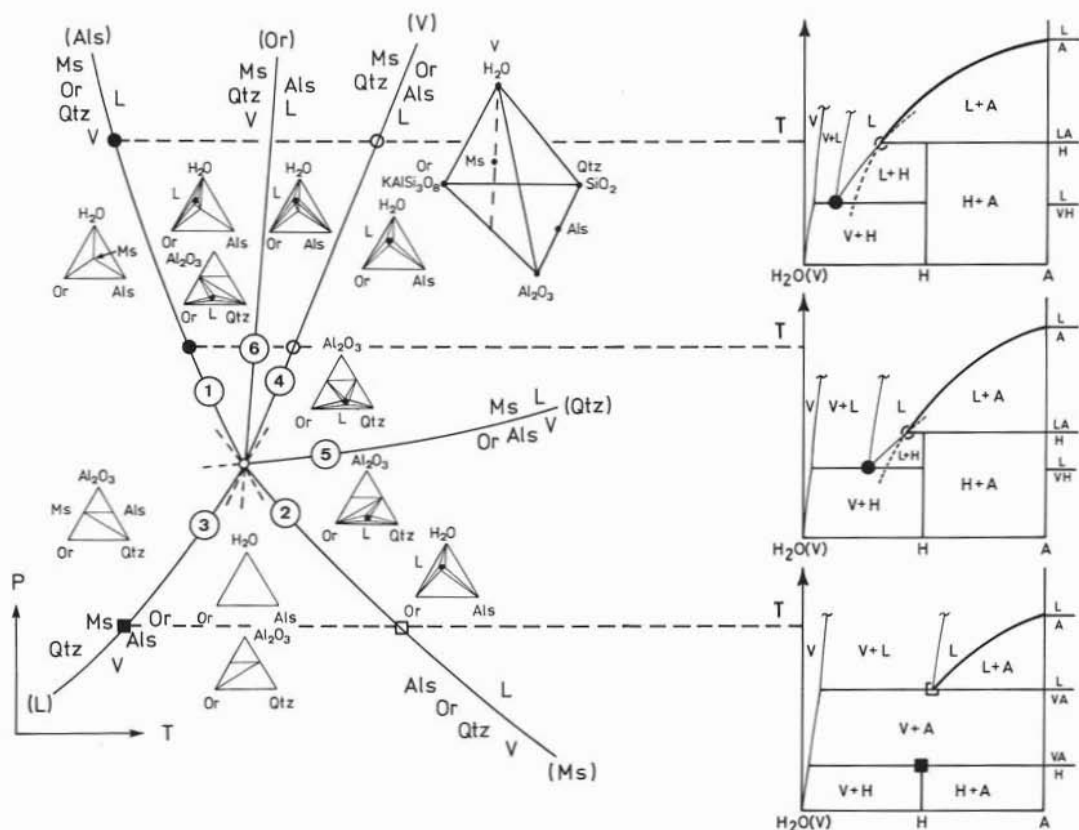


Fig. 4. — Schematic P-T diagram of muscovite + quartz dehydration melting in the system KASH (from THOMPSON and ALGOR, 1977) together with SCHEMATIC ISOBARIC T-X(H₂O) sections at three pressures. The anhydrous assemblages are denoted by A and the hydrous mineral muscovite composition (H) is arbitrarily shown with a very high water content. The schematic isobaric T-X(H₂O) sections show the evolution of peritectic and eutectic melting reactions with pressure.

has been studied experimentally by STORRE (1972) in the system $\text{KAlO}_2 + \text{Al}_2\text{O}_3 + \text{SiO}_2 + \text{H}_2\text{O}$, and that of phlogopite + Qtz via:

$$\text{Phl} + \text{Qtz} \rightarrow \text{San} + \text{Ens} + \text{H}_2\text{O-undersaturated melt} \quad (2)$$

has been studied by BOHLEN et al. (1983) in the system $\text{KAlO}_2 + \text{MgO} + \text{SiO}_2 + \text{H}_2\text{O}$.

Figure 5a shows the P-T locations of mica + quartz dehydration-melting experiments superimposed on the P-T-aH₂O melting relations for the systems $\text{Or} + \text{Qz} + \text{H}_2\text{O}$ (+/-CO₂) from BOHLEN et al. (1983). The P-T-X(H₂O) relations were calculated with reference to the dry solidus ($\text{San} + \text{Qtz} \rightarrow \text{L}$) for which an average dP/dT of 77 bars K⁻¹ and a ΔV of 0.54 Jbar⁻¹ gave

an average ΔS_{fusion} of 42 Jmol⁻¹ K⁻¹, (using a one-site ideal-solution model through the isobaric relationship $\Delta S \Delta T = RT \ln X_{\text{Or}}$). It will be noticed in Fig. 5a that the X_{w}^m surface calculated in this way when extrapolated to the H₂O-saturated solidus in $\text{Or} + \text{Qz} + \text{H}_2\text{O}$ corresponds poorly with that evaluated X_{w}^m at saturation (BURNHAM, 1982, p. 211) with a discrepancy of about 10%. Both values of X_{w}^m contours can be examined in terms of their consequences for amount of melt produced by dehydration-melting of mica.

The temperatures observed experimentally for the two mica + Qz dehydration melting reactions can be used in conjunction with the X_{w}^m contours at any pressure to estimate the amount of H₂O present in the melt through

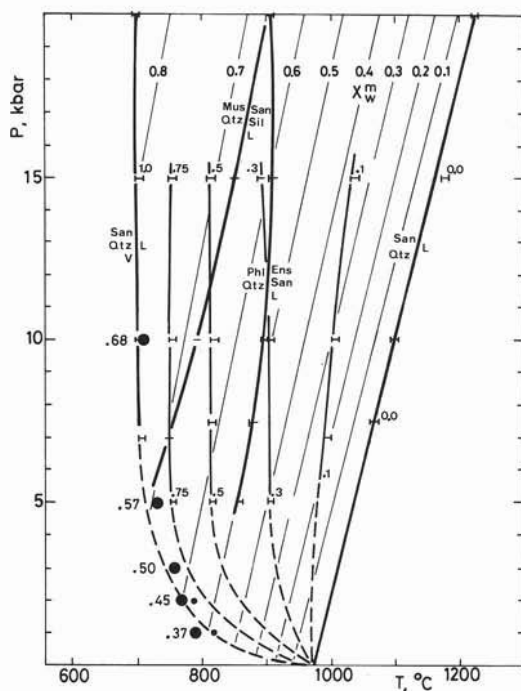


Fig. 5. — Phase relations for muscovite + quartz dehydration melting in KASH (from STORRE, 1972) and for dehydration melting in KAlO_2 -MSH (from BOHLEN et al., 1983), and for the melting of KAlSi_3O_8 (Sanidine) + SiO_2 (Qtz) + $\text{V}(\text{H}_2\text{O}-\text{CO}_2)$.

Fig. 5a) Pressure (kbar) - temperature ($^\circ\text{C}$) P-T diagram showing the experimental data, and X_w^m values for the melt calculated using an ideal solution model relative to the anhydrous solidus (see text).

The solid circles at the solidus show the values of X_w^m at saturation calculated by BURNHAM (1982, p. 211), which result in different X_w^m values in the H_2O -undersaturated region than those shown.

the dehydration melting reactions, and further to estimate the amount of melt formed for any given percentage of mica. Muscovite ($\text{KAl}_2(\text{Si}_3\text{Al})\text{O}_{10}(\text{OH})_2$) and phlogopite ($\text{KMg}_3(\text{Si}_3\text{Al})\text{O}_{10}(\text{OH})_2$) contain respectively $(18.015 / 398.311) = 4.52$ and, $(18.015 / 417.262) = 4.32$, wt% H_2O . At for example $P = 10$ Kbar (Fig. 5a), the respective dehydration-melting reactions (1) and (2) for mica + quartz dehydration melting reactions occur at about $790 \pm 10^\circ\text{C}$ and $890 \pm 10^\circ\text{C}$.

If no crystalline-solutions are involved then the dehydration-melting reactions should occur abruptly (provided there are no retarding kinetic effects) and not over a temperature interval. According to the solid

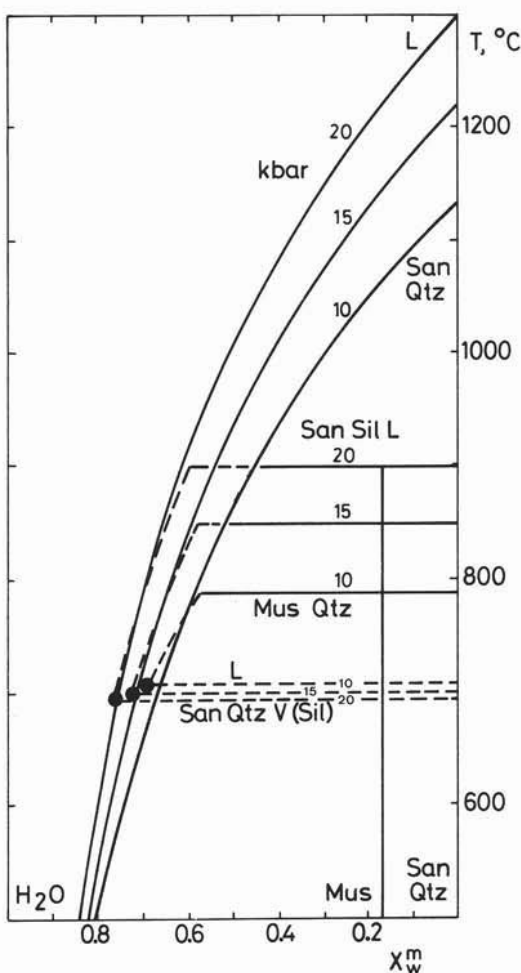


Fig. 5b) Isobaric pseudo-binary T-X (San + Qtz- H_2O) sections at 10, 15, 20 kbar, showing the liquidus surface lowering due to an ideal solution model for H_2O in the melt, and the observed dehydration melting reactions. The amount of H_2O in the melt, X_w^m , can be obtained from the horizontal line representing the dehydration-melting reaction $\text{Phl} + \text{Qtz} \rightarrow \text{San} + \text{En}(\text{enstatite}) + \text{L}$, where the San + Qtz + H_2O liquidus has been lowered by about 10 - 15°C to allow for excess MgO in the feldspar + quartz liquid. These values can be compared with those at H_2O -saturation defining the solidus $\text{San} + \text{Qtz} + \text{H}_2\text{O} \pm (\text{En}) \rightarrow \text{L}$. The amount of melt can be obtained by converting to wt% and applying the lever rule. Solid circles show the approximate amount of H_2O dissolved in the eutectic liquid at the H_2O -saturated solidii.

line contours in Fig. 5a these correspond to X_w^m values of about .68 and .52, respectively, and for the dashed line contours, X_w^m is about .58 and .42. According to the data of LUTH (1969), the composition of the

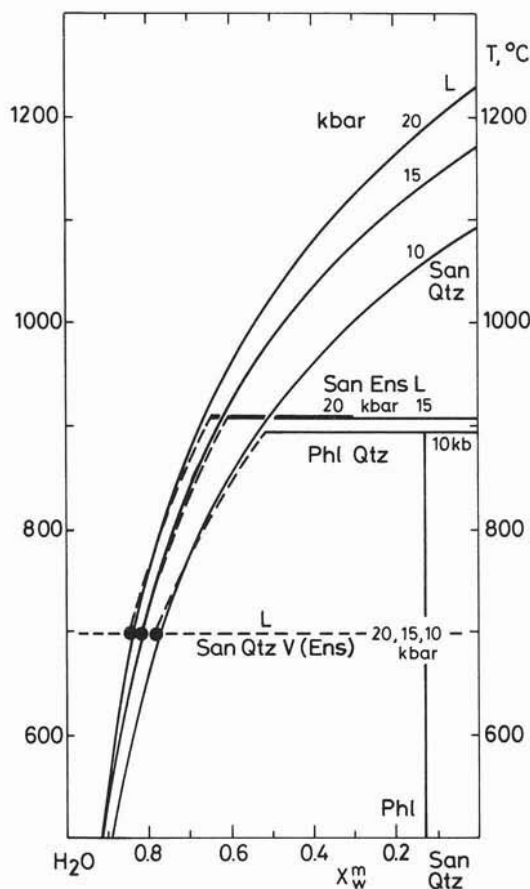
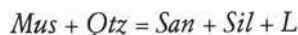
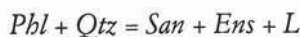


Fig. 5c) Isobaric pseudo-binary T-X (San + Qtz + H₂O) sections at 10, 15 and 20 kbar for Mus + Qtz → San + Als (sillimanite) + L.

anhydrous Or + Qz eutectic at 10 Kbar, 1140°C is about 67 wt% Or and according to BURNHAM'S (1982, p. 211) interpretations of the data of LAMBERT et al. (1969) the H₂O-saturated eutectic at 10 Kbar, 710°C is at about 58 mol% Or, which give respective gram formula weights for the mixtures of 264 and 262, on the basis of KAlSi₃O₈ + Si₄O₈. With these data, the values of X_w^m may be converted to wt% and for the above amounts of water available in the micas, the amount of melt can be calculated by simply assuming that the amount of melt is directly proportional to the amount of H₂O in the available dehydrating mica:



X_w^m	0.68	0.58
wt% H ₂ O	12.08	8.7
wt% melt	0.35	0.5



X_w^m	0.52	0.42
wt% H ₂ O	7.00	4.08
wt% melt	0.62	0.90

(per gram mica)

For quartz-feldspathic rocks it may be reasonable to assume that wt% ≈ vol% melt, in view of the density ranges involved. However, as the melts dissolve other components they will become denser.

These examples illustrate well the problems inherent in estimating the amount of H₂O-undersaturated melt formed when X_w^m values are poorly known. However, by determining the amount of melt formed in an experimental study of dehydration melting, the granite-melt model can obviously be refined.

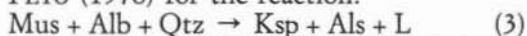
Dehydration-melting of mica in pelitic metasediments

Because of crystalline solutions and the range in chemistries of any one type of crustal rock, several dehydration-melting reactions can occur in any one rock and these will be smeared out over P-T space due to continuous reactions. Even with the little available data it is possible to predict in some approximate fashion how the melting of say metapelites will occur in terms of amount of melt formed for any given initial mineralogy over a range of P-T conditions. For metapelites the situation is only slightly more complex than the behaviour discussed in the previous section for simple systems. Firstly, dehydration-melting reactions are smeared-out in P-T space principally due to the exchanges KNa_1 in muscovite and $\text{Al}_2\text{Mg}_1\text{Si}_1$, $\text{Fe}^{+3}\text{Al}_1$ and $\text{Fe}^{+2}\text{Mg}_1$ in both muscovite and biotite.

This also permits reaction coupling involving plagioclase and AFM minerals (e.g. garnet and cordierite). Quite complex petrogenetic grids for dehydration-melting can be constructed (ABBOTT and CLARKE, 1979; THOMPSON, 1982; GRANT, 1985a, b) which at the moment

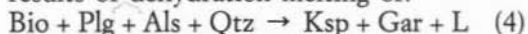
are poorly constrained experimentally.

HUANG and WYLLIE (1981), in their experimental investigation of dehydration (dry) melting of muscovite granite, noted a very high liquidus temperature (1150°C at 10kbar) defined by final disappearance of quartz but where corundum or kyanite persisted. The dry liquidus, H₂O-saturated solidus and dry solidus (dehydration melting) curves are shown in Fig. 6. Also shown are the results of PETÖ and THOMPSON (1974) and PETÖ (1976) for the reaction:



in the system KNASH, which marks the lower temperature limit of dehydration-melting with plagioclase (THOMPSON and TRACY, 1979). The dehydration-melting curve for (3) runs almost parallel to the estimated X_w^m contours from Fig. 3 for Ab + Or + Qz, such that the amount of H₂O in the undersaturated melt does not vary much with pressure.

Also shown in Fig. 6 are the experimental results of dehydration melting of:



where at 10kbar dehydration melting occurred between 760°C and 800°C for different pelite compositions (LEBRETON and THOMPSON, 1988). VIELZEUF and HOLLOWAY (1988) reported extensive dehydration-melting (40-50%) just below biotite disappearance at 860°C from 10kbar melting experiments on a natural pelite containing originally both muscovite and biotite. In synthesis experiments on a synthetic pelite with 5wt% or 2wt% added H₂O, GREEN (1976) reported biotite stability to much higher temperature ~ 900°C and ~ 1000°C, respectively.

CLEMENS (1984, p. 281) has calculated the amounts of melts produced by mica dehydration-melting at 5kbar. The data summarised in Fig. 6 are used here to calculate the amount of melt formed at 10kbar for his hypothetical *medium-grade pelite* (44% Qz, 23% Plg, 33% Mus, by weight) and *high-grade pelite* (35wt% Qz, 20% Plg, 5% Kfs, 10% Sil, 25% Bio, 5% Gar). For muscovite-dehydration melting intervals at 10kbar between 740°C to 765°C, the corresponding X_w^m values are .60 and .57, and for a gram formula weight of the melt (gfw_m = 260)

leads to 9.4wt% and 8.1wt%, respectively. Thus 33wt% Mus yields ($33 \times 4.5 = 1.485$ gm H₂O), which leads to $1.485/9.4 = 15.8$ or $1.485/8.1 = 18.33$ wt% melt, respectively. For biotite-dehydration melting intervals of 790°C to 840°C at 10kbar, the corresponding X_w^m values are .54 and .43 (leading to 7.5 and 4.96wt%, respectively). Thus 25wt% Bio yields ($25 \times 4.3 = 1.075$ gm H₂O), which leads to $1.075 / 7.5 = 14.33$ and $1.075/4.96 = 21.6$ wt% melt, respectively.

These values can be used to assess the amount of melt formed at any particular temperature (Fig. 7) and differ from those calculated by CLEMENS (1984) only because of the X_w^m values used in Fig. 6. The mica dehydration-melting reactions have been shown over distinct temperature intervals in Fig. 7 to illustrate the continuous nature of the melting reactions. In both cases the amount of dehydration-melt produced is lower than the values calculated to disaggregate close-packed spheres (~ 35 vol%, see summary diagram by WICKHAM, 1987, p. 282).

The rest of the melting path (a) is only constrained by the temperature of the muscovite-granite «dry» liquidus near 1240°C (HUANG and WYLLIE, 1981) and will not necessarily be continuous as shown when successive minerals are dissolved in the higher temperature melts. For the schematic version shown by the solid line (path a) significant further temperature increases are needed to produce more melt (see also CLEMENS and VIELZEUF, 1987). PIWINSKI (1975, p. 227 and JOHANNES, 1985, p. 73) have estimated the amount of glass at different temperatures from melting of natural granitoids at H₂O-saturation, and their data indicate a form as schematically represented by the dashed line (path b) in Fig. 7. The actual form of the liquidus surface depends upon the temperature of specific cotectics and the degree of solubility of additional components in the melt. Clearly, path b would result in generation of higher melt fractions at lower temperatures. As the amount of melt generated at particular temperatures is of great importance for melt extraction, further experimental and theoretical studies are clearly needed.

Dehydration melting of a two mica-bearing metapelite would show two distinct melting pulses in Fig. 7 but the total amount of melt is still proportional to the amount of mica, which is between .48 to .55 and .57 to .86wt% melt per gm of muscovite and biotite respectively.

The amount of melt generated at any pressure depends upon how the dP/dT of the dehydration-melting reaction changes in relation to the X_w^m contours, and as with H_2O -saturated melting the amount of melt is still dependent both upon temperature and amount of H_2O available. Thus while micas

contain about 4.3 - 4.5wt% H_2O and undergo dehydration melting at reasonably low temperatures, the amount of H_2O in the melt is high. Amphibolites contain less H_2O (1-2wt%) but because they dehydrate at higher temperatures where X_w^m is lower, they will produce proportionally more melt, albeit at higher temperature. In any case much higher temperatures are needed for amphibole dehydration-melting than for biotite than muscovite, thus metapelites will generally be more «fertile» (in the sense of amount of melt able to be generated) than amphibolites at any temperature (see also CLEMENS and VIELZEUF,

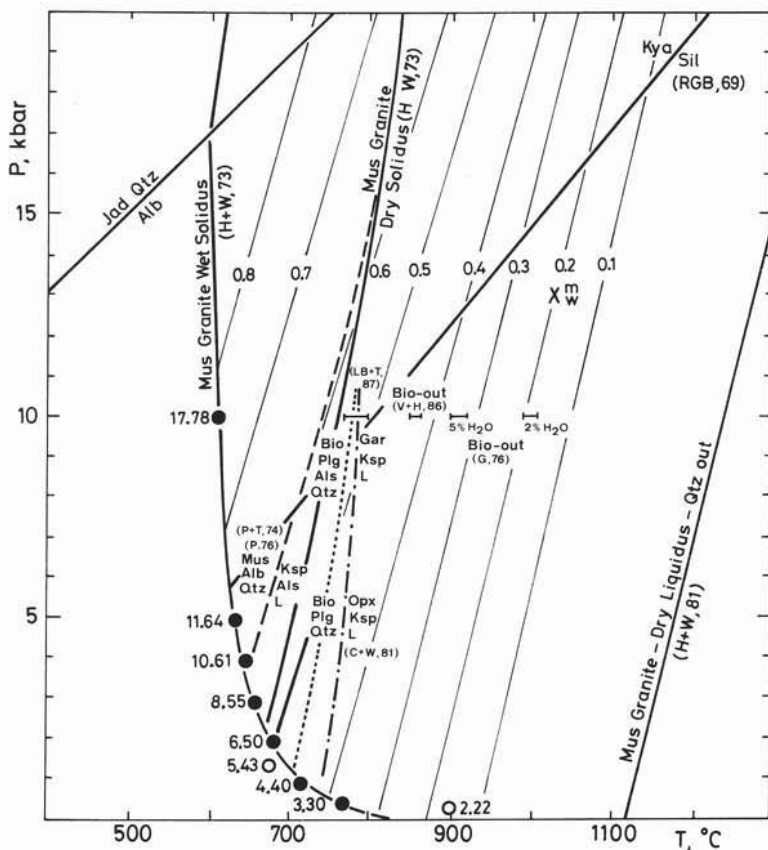


Fig. 6. — P-T diagram showing the wet solidus, dry solidus and dry liquidus for a muscovite-granite (HUANG and WYLLIE, 1981), together with the X_w^m contours for $Ab + Or + Qz + H_2O$ (Fig. 3) and several mica dehydration melting reactions. The reaction (dashed line) $Mus + Alb + Qtz \rightarrow Ksp + Als + L$ (PETÖ and THOMPSON, 1974; PETÖ, 1976) marks the lower T limit of plagioclase reactions (THOMPSON and TRACY, 1979). The brackets at 10kbar show the reaction (dotted line) $Bio + Plg + Als + Qtz \rightarrow Gar + Ksp + L$ beginning at about 790°C (LE BRETON and THOMPSON, 1988) and ending at about 860°C (VIELZEUF and HOLLOWAY, 1986). The other brackets show the disappearance of biotite at 5% and 2% added water to synthetic pelite (GREEN, 1976). The calculated dehydration melting reaction (dot-dashed line) $Bio + Plg + Qtz \rightarrow Opx + Ksp + L$ is from CLEMENS and WALL (1981). Kyanite-sillimanite phase relations are from RICHARDSON et al. (1969).

1987). The compositional variation of liquids produced by dehydration melting of both pelites and amphibolites will be discussed further below.

Dehydration-melting of amphibolites

Melting of amphibolites has been discussed by BURNHAM (1967, p. 64; 1979a, p. 85), where the reference solidi are usually governed by plagioclase + /—quartz melting reactions. The experimental results obtained

the basalts melted by HELZ (1976) at $\text{PH}_2\text{O} = 5\text{ kbar}$, liquid compositions between 700 and 1000°C coexist initially with plagioclase and hornblende, then pyroxene. The enlargement of the compositional space around the feldspar composition (Fig. 8b) shows the peraluminous nature of «granitic» melts produced by amphibolite-melting. This results in amphibole becoming less aluminous with successive melting until clinopyroxene appears (as shown in the model system CMASH, ELLIS and THOMPSON, 1986). With

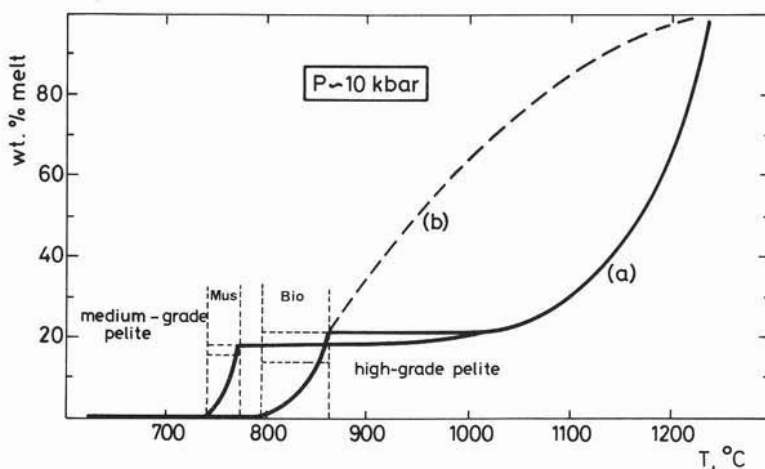


Fig. 7. — The amount of melt as a function of temperature at about 10 kbar for the dehydration-melting of medium- and high-grade pelites discussed by CLEMENS (1984, p. 281), where the dehydration-melting temperature intervals and X_w^m are obtained from Fig. 6, and the rest of the diagram, although highly schematic is based upon Fig. 3 of HUANG and WYLLIE (1981, p. 1052) for path *a*, and upon PIWINSKI (1975, p. 227) and JOHANNES (1985, p. 73) for path *b*.

by HELZ (1976) at 5 kbar for H_2O -saturated melting of three basalts, have been replotted in Fig. 8 in ACF-deluxe coordinates (see O'HARA, 1976, p. 110; J.B. THOMPSON, 1981, p. 175). The differences with conventional ACF diagrams can be seen in Figs. 10 and 11 of ELLIS and THOMPSON (1986). In ACF-deluxe, the molar groupings of $A (= \text{Al}_2\text{O}_3 + \text{Na}_2\text{O} + \text{K}_2\text{O})$ and $C (= \text{CaO} + 2\text{Na}_2\text{O} + 2\text{K}_2\text{O})$ result in all feldspar components plotting at a single point, which at quartz and H_2O saturation defines the entire «granite» system. Thus the diagram (Fig. 8a) shows divergence of evolving anatectic melts as excess Al_2O_3 , FeO, MgO and CaO become progressively dissolved. For

increasing temperature (at around 1000°C, $\text{PH}_2\text{O} = 5\text{ kbar}$; HELZ, 1976), the melts become metaaluminous then eventually wollastonite (or diopside) normative. It is clear from HELZ's (1976) results that even at 1000°C at H_2O -saturation, only about 12 mol% of non-granitic components are dissolved in the melts.

Several relevant questions arise from these observations, 1) does the melt contain smaller amount of non-granitic components when H_2O -undersaturated?; 2) how do the melt compositions vary when micas are involved?; and 3) how does the melting of mica or amphibole effect the Ab:Or:An:Qz composition of the melt and hence the rock

classification (remembering that mica contains latent *Or* and amphibole latent *An* and *Ab*)?

BROWN and FYFE (1970) reported the results of dehydration melting for the addition of 10 or 50wt% of either muscovite (M), biotite (B) or hornblende (H), to natural granite (G) and diorite (D). Their recalculated results of melt compositions are shown in the enlarged region of the ACF-deluxe diagram in Fig. 8c. The divergence of their melt compositions from the «granite» system (Fig. 8c) are similar to those observed by HELZ (1976: shown in Fig. 8b). This could be taken to indicate that both H_2O -undersaturated and H_2O -saturated melts contain similar amounts of non-quartzofeldspathic components, although presumably less in the lower amount of dehydration melt at any temperature. However, data is insufficient to indicate whether or not, the excess components CaO , FeO , MgO and Al_2O_3 dissolve equally in granitic melts at all pressure and aH_2O .

The glass compositions reported by BROWN and FYFE (1970), HELZ (1976), and NANEY

(1983) have been plotted in a mol% *An-Ab-Or* diagram (see KILINC, 1972) in Fig. 9.

The melt compositions for NANEY's (1983, p. 1000) synthetic granite at $PH_2O = 8kbar$, lie close to the H_2O and quartz-saturated eutectic in $Ab + Or + An + Qtz + H_2O$ (WINKLER, 1979) and show with increasing temperature the influence of coexisting clinopyroxene, biotite then orthopyroxene. NANEY's (1983, p. 1000) melt compositions from synthetic granodiorite show the influence of coexisting biotite, epidote then hornblende with increasing temperature. The melt compositions plot within O'CONNOR's (1965, see KILINC, 1972) granodiorite field.

The melt compositions reported by BROWN and FYFE (1970) for granite and diorite show clearly the effects of addition of hornblende, biotite or muscovite, and plot in the vicinity of the H_2O -saturated cotectic at the appropriate pressures.

The melt compositions reported by HELZ (1976, Figs. 4a-d) for H_2O -saturated melting of various basalts (amphibolites) show well the effects of progressive hornblende resorption

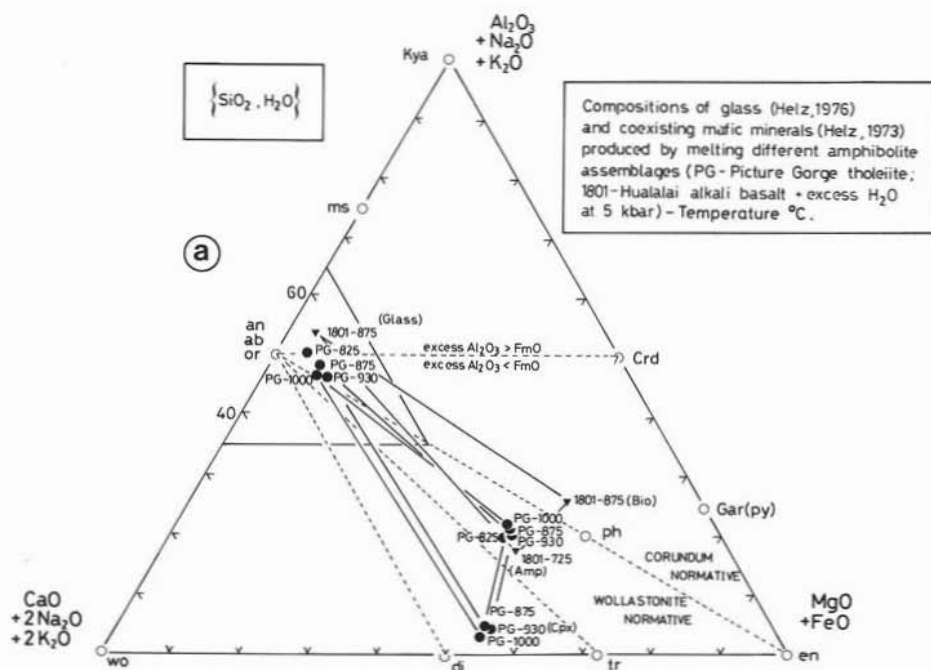


Fig. 8. — a) ACF deluxe projection from quartz and H_2O showing glass composition and coexisting minerals produced by H_2O -saturated melting of amphibolites at 5kbar (HELZ, 1976).

on melt evolution. The hornblende compositions have been plotted simply by considering $(2\text{-CaO})/2$, molar, as this is an approximate representation of the $\text{CaAlNa}_1\text{Si}_1$ vector in amphibole. However,

the NaAlSi_1 vector in amphibole results in displacement of the projected composition (from quartz) towards albite.

In all cases the melts are peraluminous, except at the highest temperatures for melting

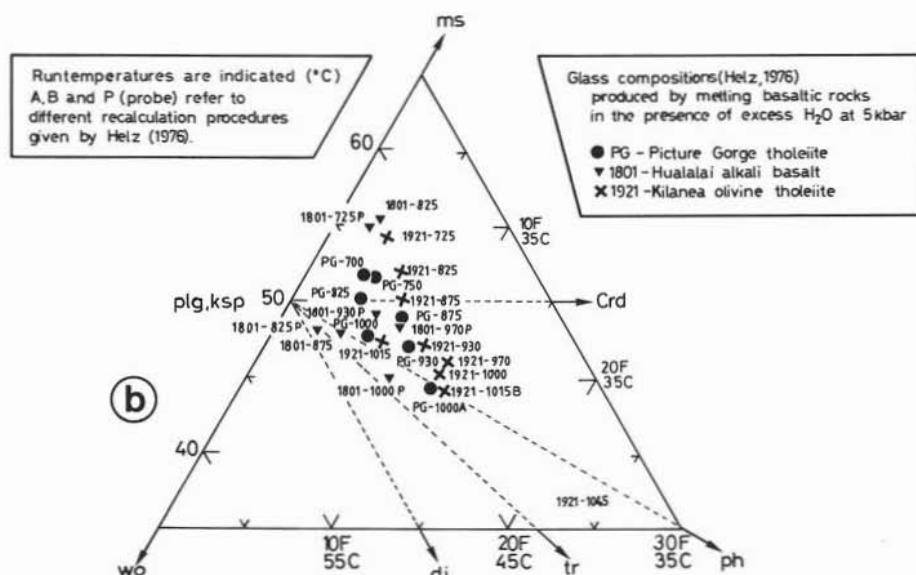


Fig. 8b) Enlargement of the area around the granite minimum showing the peraluminous and metaluminous nature of amphibolite melt at $\text{PH}_2\text{O} = 5$ kbar.

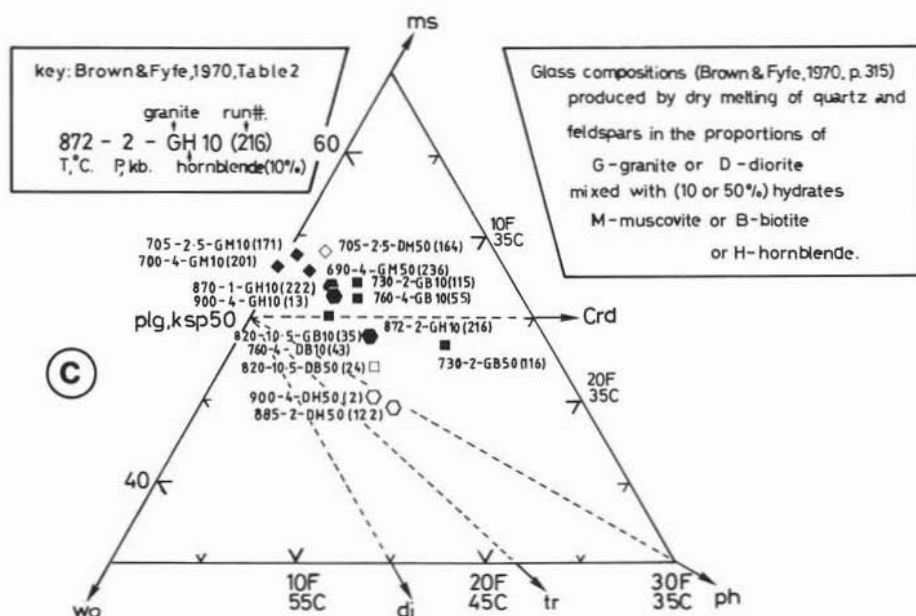


Fig. 8c) Glass compositions produced by BROWN and FYFE (1970) from dehydration-melting of muscovite, biotite or hornblende with mixtures of quartz and feldspar at various pressures.

of amphibolites (see ELLIS and THOMPSON'S, 1986, Figs. 10 and 11, representation of HELZ'S, 1976 data) when wollastonite (diopside) normative melts are reached. The data plotted in Fig. 9 show well the influence of the composition of the hydrated mineral undergoing dehydration melting, on the melt compositional evolution.

Compositional evolution of liquids produced by dehydration melting of common crustal rock types

With progressive melting not only do most crustal rocks types produce pseudo-granitic liquids even through dehydration-melting, their compositions evolve progressively with increasing temperature in ACF-deluxe coordinates (Fig. 8) and in Ab + Or + An space (Fig. 9). The compositional evolution depends upon the amount of quartzo-

feldspathic components in the original rock as well as the amounts and compositions of muscovite, biotite and amphibole, because the dehydration melting reactions involve both feldspathic and ACF-deluxe components. Melting of both muscovite and biotite release respectively Al_2O_3 and $(\text{FeO} + \text{MgO})$ components, and KAlSi_3O_8 , which can result in orthoclase saturation in melts from rocks in which alkali-feldspar was not previously present. Depending upon the actual amphibole compositions melting, the amount and composition of plagioclase is effected by $\text{NaSiCa}_1\text{Al}_1$ exchange, as is the melt.

Possible evolution of a range of melts towards or away from the «granite» minimum composition can be seen with aid of the ACF-deluxe projection in Fig. 10a, where the compositional ranges of common minerals and rock-types are also shown. The schematic cotectic surfaces are based upon case A of

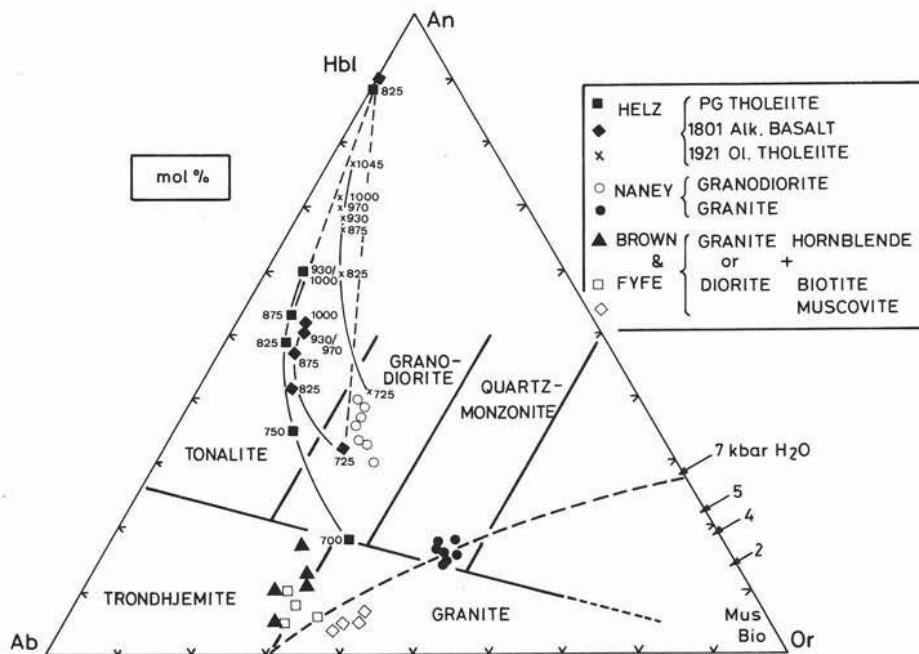


Fig. 9. — Melt compositions obtained in various experimental studies plotted in molar Ab-Or-An units. Those from HELZ (temperatures indicated in °C) and from Naney were obtained at H_2O -saturation, those from BROWN and FYFE without excess H_2O . All melts are corundum normative with the exception of those produced by amphibolite + H_2O melting above about 1000°C (see ELLIS and THOMPSON'S, 1986; FIGS. 10 AND 11; REPRESENTATION OF HELZ'S, 1976; data). Also shown are coexisting amphiboles along the $\text{NaSiCa}_1\text{Al}_1$ vector. Both muscovite and biotite plot near Or. Several experimental determinations of the ternary cotectic in $\text{Ab} + \text{Or} + \text{An} + \text{H}_2\text{O}$ are shown (WINKLER, 1979). The compositional fields of some siliceous plutonic rocks are also presented (from KLINIC, 1972; after O'CONNOR, 1965).

CAWTHORN and BROWN (1976, p. 471) but are drawn to incorporate, as best as possible, the data available from dehydration-melting studies near 10kbar. Reactions involving clinopyroxene (Cpx) and amphibole (Hbl)

with feldspathic liquids are shown as peritectic and those among muscovite (Mus) and biotite (Bio) as eutectic. As noted above the diagram strictly applies at quartz and H_2O -saturation, but nevertheless this «illegal»

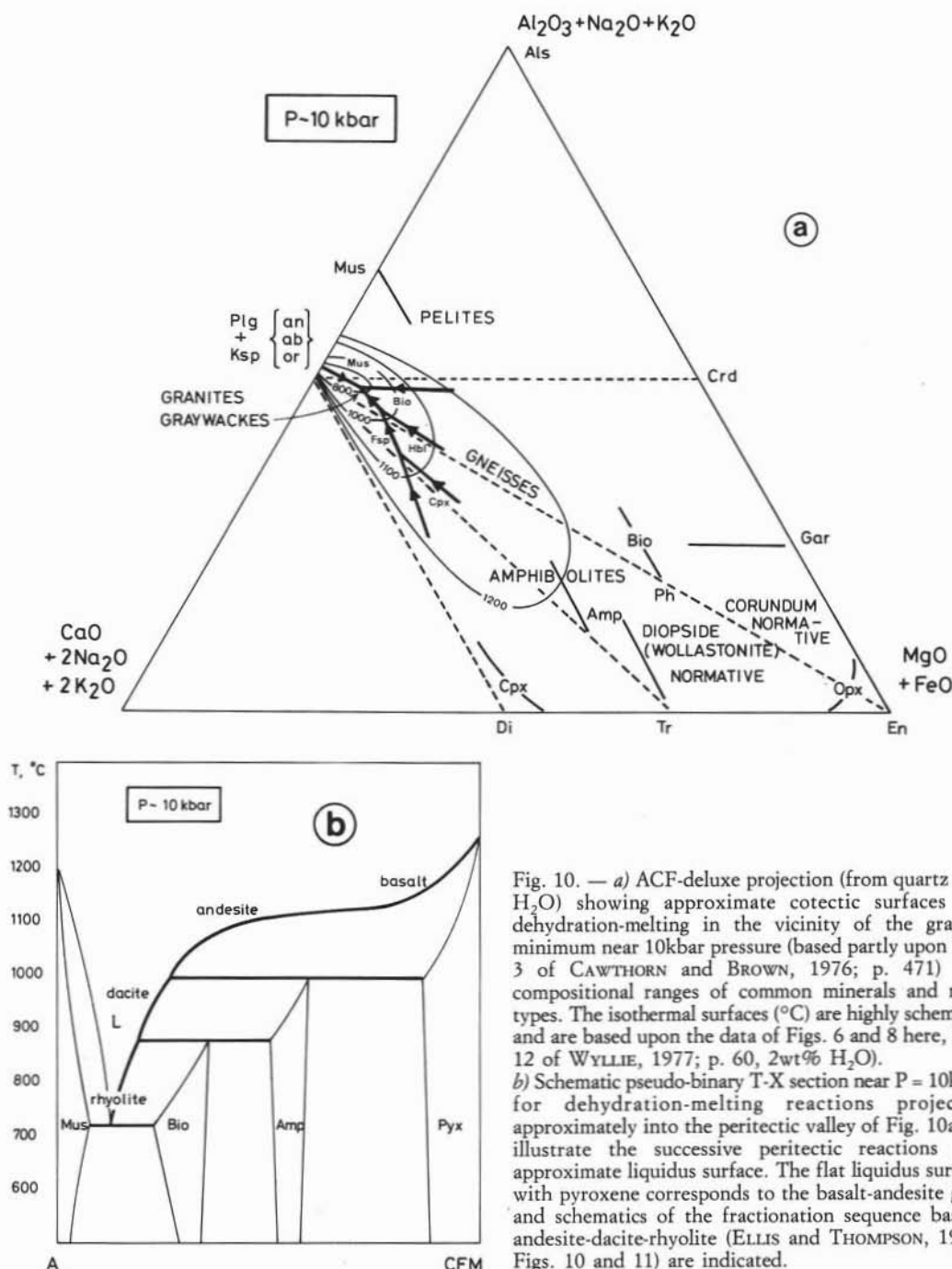


Fig. 10. — a) ACF-deluxe projection (from quartz and H_2O) showing approximate cotectic surfaces for dehydration-melting in the vicinity of the granite minimum near 10kbar pressure (based partly upon Fig. 3 of CAWTHORN and BROWN, 1976; p. 471) and compositional ranges of common minerals and rock types. The isothermal surfaces (°C) are highly schematic and are based upon the data of Figs. 6 and 8 here, Fig. 12 of WYLLIE, 1977; p. 60, 2wt% H_2O).

b) Schematic pseudo-binary T-X section near $P = 10$ kbar for dehydration-melting reactions projected approximately into the peritectic valley of Fig. 10a, to illustrate the successive peritectic reactions and approximate liquidus surface. The flat liquidus surface with pyroxene corresponds to the basalt-andesite gap, and schematics of the fractionation sequence basalt-andesite-dacite-rhyolite (ELLIS and THOMPSON, 1986; Figs. 10 and 11) are indicated.

projection can also illustrate some aspects of H_2O undersaturated liquids that also dissolve quartz or feldspar early (not always the case, see HUANG and WYLLIE, 1981). The approximate isothermal surface shows also likely shape of valleys and ridges in the complex T-X space. Fig. 10b has been constructed as an approximate pseudo-binary T-X section along the peritectic valley of Fig. 10a. Although highly schematic in that the feldspathic components are not shown, the diagram resembles in some respects T-X diagrams drawn for varying SiO_2 content (eg. WYLLIE, 1977, Figs. 12 and 13). The actual peritectic valley will be much more complex because of smearing due to continuous reactions. The intention is to show how the dT/dX of the liquidus surface in a very complex composition space varies. Especially important are the very steep dT/dX values near the Mus + Bio + Fsp (pseudo)-eutectic which strongly constrains the compositional evolution of non-quartzofeldspathic components in the melts to a small range even up to about $1000^\circ C$. The shallow dT/dX of the liquidus surface towards mafic compositions means that above about $1100^\circ C$ (for the conditions of Fig. 10b) rapid compositional changes would occur for either anatectic liquids produced from amphibolites or for the crystallisation of basalt to andesite (ELLIS and THOMPSON, 1986, Figs. 10, 11).

Dehydration-melting reactions at different pressure and sequence of anatexis at various crustal depths

Earlier considerations of dehydration-melting reactions had suggested that they had steep positive dP/dT to at least 20 kbar (BROWN and FYFE, 1970; BURNHAM, 1967, Fig. 2.9; 1979a, Fig. 3.4). Calculations by CLEMENS and WALL (1981, Fig. 8) and by CLEMENS (1984, Fig. 2) indicated that some biotite dehydration-melting reactions that produced garnet (curve *c* in Fig. 11) resulted in backbending of the curves at relatively low-pressure (eg. 3-4 kbar). A similar proposal has been put forward by PERCIVAL (1983, Fig. 5) for amphibolite melting producing garnet (curves *e* and *f* in Fig. 11). Backbending occurs

because the reactions have small ΔV_{solids} and the production of dense minerals, such as garnet, and the high compressibility of H_2O as vapour or dissolved in the melt, cause $\Delta V_{\text{reaction}}$ to go from positive to negative. Experimental data has shown that muscovite dehydration-melting has similar positive dP/dT until at least 20 kbar (curves *a-b* in Fig. 11).

If we consider the melting sequences at various pressures implied by curves (Mus (*a*)-Bio (*c*) and Hbl (*e-f*) then below about 8 kbar the dehydration-melting sequence would first involve Mus then Bio in pelitic rocks then Hbl in amphibolites. Whereas at 15 kbar, Bio would melt in metapelites then Hbl in amphibolites then Mus in pelites. If true, this would provide another important diagnostic characteristic of high pressure magmatites, in addition to individual mineral stabilities. However, the quantities of anatectites from amphibolites for the curves (*e-f*) would also be restricted because of the lower X_w^m at these pressures.

Before looking too hard in the field for such characteristic migmatites formed by dehydration-melting at high pressures, some limited but important additional experimental constraints should be considered. Firstly, dehydration-melting of a natural biotite assemblage according to reaction (4) did not apparently show backbending 10 kbar (LE BRETON and THOMPSON, 1988) possibly because the Bio is stabilised to higher temperature in nature due to Ti substitution. Hence backbending of the dehydration-melting curve would not occur until much higher pressure (e.g. curve *d* in Fig. 11). Even here biotite might undergo dehydration-melting before (or at the same time) as muscovite in high-pressure migmatites.

Little experimental information is available for dehydration-melting of amphibolites. In the simple system CMASH, ELLIS and THOMPSON (1986, p. 113) noted that dehydration-melting occurred between $900-950^\circ C$. With natural amphibolite mineralogy, RUSHMER (1987) observed dehydration-melting to occur between 925 and $950^\circ C$ at 8 kbar. Clearly, the effects of Ti in stabilising amphibole and Fe in

stabilising garnet need further investigation to show in which pressure-range backbending of amphibolite dehydration-melting curves will occur for the whole range of basaltic compositions.

Control on crustal anatexis

The simple considerations outlined above demonstrate how the proportions of melt produced by dehydration-melting of common crustal rock types can be crudely estimated

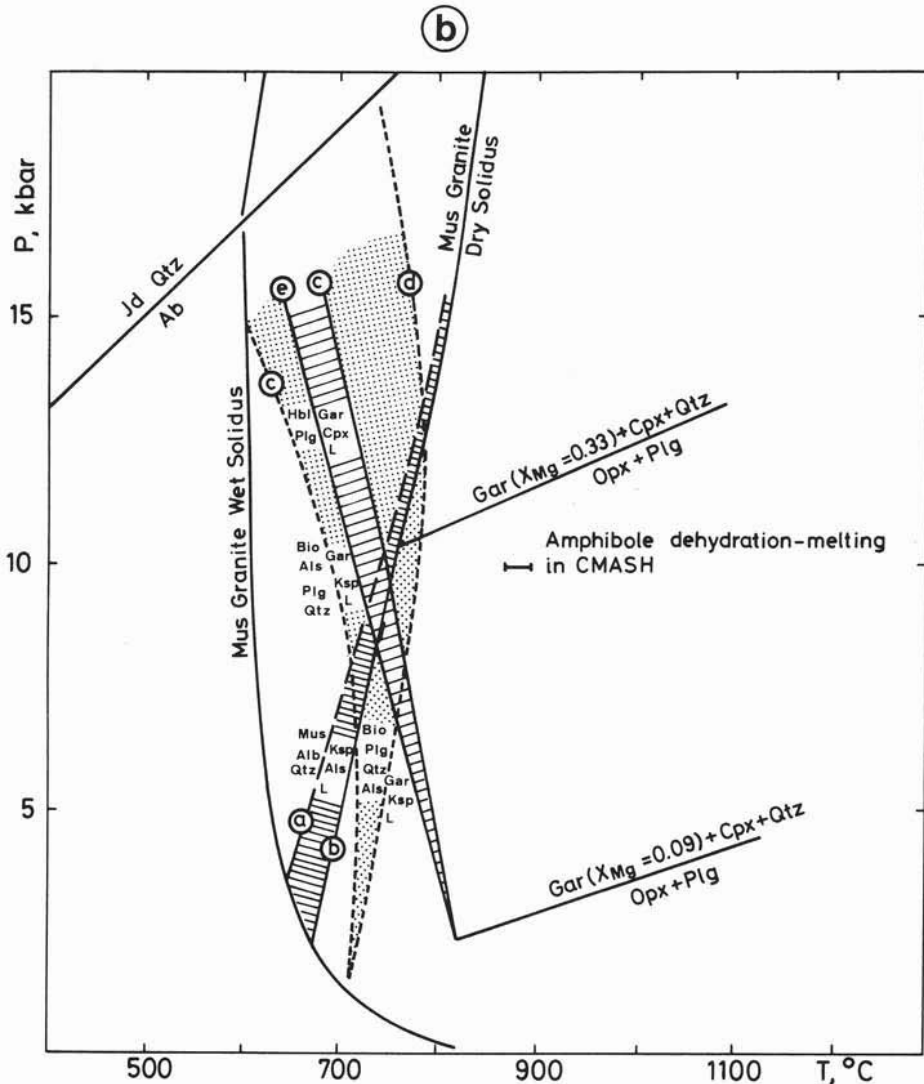


Fig. 11. — P-T diagram showing proposed backbending of dehydration-melting reactions for various mineral assemblages. The muscovite + quartz reactions (Fig. 6) have $+dP/dT$ at least 20kbar. The calculated backbending for biotite (CLEMENS and WALL, 1981; CLEMENS, 1984; Fig. 2) and amphibole (PERCIVAL, 1983; Fig. 5) dehydration-melting reactions, labelled as c-d (stippled range) and e-f (dashed range), apparently show backbending due to formation of the dense assemblage with garnet (compositions given in X_{Mg} from PERCIVAL, 1983). If the calculated curves are correct, then melting at about 5kbar would show successive dehydration-melting of muscovite then biotite then hornblende, whereas at high pressure (say 15kbar) amphibolites would melt before some pelites. Recent experimental data however indicate that these dehydration melting curves apparently do not backbend within crustal depths.

at any pressure and temperature. Several other major aspects should be considered before a general model for crustal melting can be developed, they include: — nature of heat source for melting and the distribution of latent heat with temperature, H_2O -migration to the melting site and diffusion of H_2O through the anatectic melt, mechanisms of melt segregation and the geodynamics of granite intrusion. As some aspects have been discussed elsewhere only a short discussion will be included here.

Heat sources for crustal melting

Two commonly proposed causes for anatexis include high-temperature intrusions and the intersection of the appropriate solidi by metamorphic pressure-temperature-time (PTt) paths.

Following the calculations by JAEGER (1957) of temperatures around cooling magma bodies, it appears that each volume of crustal melt requires approximately the same volume of mafic melt to generate it (BURNHAM, 1979, p. 97; ENGLAND and THOMPSON, 1986, p. 92) and that even a 10 km sized mafic pluton has solidified in about 10^5 years, consequently leaving only a short time for effective anatexis. If external H_2O sources are proposed (H_2O -saturated rather than dehydration-melting) then this H_2O must diffuse to the melting site also during the time when the heat source is active.

Some calculated PTt paths following crustal thickening pass above the appropriate dehydration melting solidi for common crustal rock types (THOMPSON and ENGLAND, 1984; ENGLAND and THOMPSON, 1986) and provide a feasible means of crustal anatexis without necessarily requiring an augmented heat supply from mantle magma. Not yet well understood are the effects of latent heat on PTt paths (but see RIDLEY, 1986) and how this will effect melt fraction.

H_2O -migration to the melting site and through anatectic melts

H_2O -diffusivities through high-grade metamorphic rocks are poorly known, but

BRADY (1983) has proposed a value of D of about $10^{-9} m^2 s^{-1}$. For a characteristic diffusion length defined by $x^2 = 4Dt$, distances penetrated as a function of time can be easily calculated as order of magnitude estimates:

x (m)	10^3 (1km)	10^2	10^1	10^0 (1m)	10^{-1} (1cm)
$\sim t$ (years)	10^7	10^5	10^3	10^1	10^{-1}

which, given the above time constraints on the cooling of mafic plutons (10 km size in about 10^5 years), means that H_2O can only diffuse on the order of 100 m. This simple calculation enables the evaluation of the maximum amount of H_2O that could be available for H_2O -saturated melting of any particular high-grade metamorphic rock.

Diffusivities of H_2O through obsidian glasses and melts (see summary by HOFMANN, 1980, p. 401) reveal values of D about $10^{-10.5} m^2 s^{-1}$ at $1000^\circ C$ and $10^{-12.5} m^2 s^{-1}$ at $750^\circ C$. Using the characteristic diffusion equation above provides the following order of magnitude estimates:

x (m)	10^4	10^3	10^2	10^1	10^0
$\sim t$ (years) ($750^\circ C$)	10^{12}	10^{10}	10^8	10^6	10^4
$\sim t$ (years) ($1000^\circ C$)	10^{10}	10^8	10^6	10^4	10^2

These simple calculations reveal that the rate limiting step is not the diffusion of H_2O to the melt *but through the melt* (SHAW, 1965, 1974; BURNHAM, 1967, p. 47). This can be viewed as a physical argument in favour of dehydration-melting, where the H_2O released from hydrous minerals only needs to travel short distance through melts at dispersed melting sites. Thereafter a moving melt carries any dissolved H_2O with it, until the solidus is crossed and boiling occurs.

Mechanisms of melt segregation and separation into intrusions

WICKHAM (1987) has discussed extensively some of the problems associated with segregation and separation of anatectic melts. Not yet fully understood is the role of shear deformation (ARZI, 1978; VAN DER MOLEN and PETERSON, 1979) on melt segregation. This becomes especially important for the segregation of the low-melt fractions produced

by dehydration-melting, even though JUREWICZ and WATSON'S (1985) measurements of dihedral angles of 44-60° in dry granite systems implies that such melts would form an interconnected granular film capable of being extracted. Because H_2O diffusion is quite slow through granite melts, on short anatectic time scales, viscosity and density of even thin melt layers will not be homogeneous. One simple conclusion might be in fact that migmatites are unsuccessful (aborted) granites. Clearly further considerations of the physical aspects of magma migration open a whole new and necessary field of textural, mineralogical, chemical and isotopic investigations of migmatites and plutons.

Acknowledgements. — I am grateful to Prof. C.A. Ricci and the organisers of the SIMP for the invitation to the meeting in Siena.

Discussions with or review by Nicole le Breton, John Clemens, Ron Frost and Daniel Vielzeuf were most helpful. I am grateful to U. Stidwill for typing and to B. Bühlmann for drafting. Financial support by the Schweizerische Nationalfonds and the ETH are gratefully acknowledged.

REFERENCES

- ABBOTT R.N. JR., CLARKE D.B. (1979) - *Hypothetical liquidus relationships in the subsystem Al_2O_3 -FeO-MgO projected from quartz, alkali-feldspar and plagioclase for $a(H_2O) \leq 1$* . Can. Mineral., 19: 549-560.
- ARZI A.A., (1978) - *Critical phenomena in the rheology of partially melted rocks*. Tectonophysics, 44, 173-84.
- BOHLEN ST.R. et al. (1983) - *Stability of phlogopite-quartz and sanidine-quartz: A model for melting in the lower crust*. Contrib. Mineral. Petrol. 83: 270-277.
- BRADY J.B. (1983) - *Intergranular diffusion in metamorphic rocks*. Amer. J. Sci., 283-A, p. 181-200.
- BROWN G.C., FYFE W.S. (1970) - *The Production of Granitic Melts during Ultrametamorphism*. Contrib. Mineral. Petrol. 28: 310-318.
- BURNHAM C. WAYNE (1967) - *Hydrothermal fluids at the magmatic stage*. In: Geochemistry of Hydrothermal Ore Deposits, H.L. Barnes, ed., New York: Holt, Rinehart and Winston, p. 34-67.
- BURNHAM C. WAYNE (1979a) - *Magmas and Hydrothermal Fluids*. In: Geochemistry of Hydrothermal Ore Deposits, H.L. Barnes, ed., New York: Holt, Rinehart and Winston, 2nd edition, p. 71-136.
- BURNHAM C. WAYNE (1979b) - *The importance of volatile constituents*. In: H.S. Yoder (Editor), The Evolution of the Igneous Rocks - Fiftieth Anniversary Perspectives. Princeton, N.J., 439-482.
- BURNHAM C. WAYNE (1982) - *The nature of multicomponent aluminosilicate melts*. In: D. Rickard and F.E. Wickman (Editors), Chemistry and Geochemistry of solutions at high temperatures and pressures. Oxford, Pergamon Press 197-229.
- BURNHAM C. WAYNE, DAVIS N.F. (1971) - *The role of H_2O in silicate melts: I. P-V-T relations in the systems $NaAlSi_3O_8$ - H_2O to 10 kilobars and 1000°C*. Amer. J. Sci., 270, p. 54-79.
- BURNHAM C. WAYNE, DAVIS N.F. (1974) - *The role of H_2O in silicate melts: II. Thermodynamic and phase relations in the system $NaAlSi_3O_8$ - H_2O to 10 kilobars, 700° to 1100°C*. Amer. J. Sci., 274, p. 920-940.
- CATHWORTH R.G., BROWN P.A. (1976) - *A model for the formation and crystallization of corundum-normative calc-alkaline magmas through amphibole fractionation*. J. Geol., 84, 467-476.
- CLEMENS J.D. (1984) - *Water contents of silicate to intermediate magmas*. Lithos, 17, 273-287.
- CLEMENS J.D., WALL V.J. (1981) - *Origin and crystallization of some peraluminous (S-Type) granitic magmas*. Can. Mineral. 19: 111-131.
- CLEMENS J.D., VIELZEUF D. (1987) - *Constraints on melting and magma production in the crust*. Earth Planet. Sci. Letts. 86, 287-306.
- ELLIS D.J., THOMPSON A.B. (1986) - *Subsolidus and Partial Melting Reactions in the Quartz-excess $CaO + MgO + Al_2O_3 + SiO_2 + H_2O$ System under Water-excess and Water-deficient Conditions to 10 kb: Some Implications for the Origin of Peraluminous Melts from Mafic Rocks*. J. Petrol. Vol. 27, Part 1, 91-121.
- ENGLAND P.C., THOMPSON A.B. (1986) - *Some thermal and tectonic models for crustal melting in continental collision zones*. From: Coward M.P. Ries A.C. (Editors) Collision Tectonics, Geological Society Special Publication N° 19, 83-94.
- GRANT J.A. (1985) - *Phase equilibria in low-pressure partial melting of pelitic rocks*. Amer. J. Sci., 285, p. 409-435.
- GRANT J.A. (1985) - *Phase equilibria in partial melting of pelitic rocks*. Ashworth J.R. (Eds.) Migmatites: Glasgow, Blackie and Son, 86-144.
- GREEN T.H. (1976) - *Experimental generation of cordierite- or garnet-bearing granitic liquids from a pelitic composition*. Geology, 4, 85-88.
- HARRIS P.G., KENNEDY W.Q., SCARFE C.M. (1970) - *Volcanism versus plutonism - the effect of chemical composition*. In: Mechanism of Igneous Intrusion, G. Newall and N. Rast. Geol. J., Spec. Issue 2, 187-200.
- HELZ R.T. (1976) - *Phase relations of basalts in their melting ranges at $PH_2O = 5$ kb. Part I. Melt compositions*. J. Petrology, 17, N° 2, p. 139-193.
- HUANG W.L., WYLLIE P.J. (1981) - *Phase Relationships of S-Type Granite with H_2O to 35 kb: Muscovite Granite from Harney Peak, South Dakota*. J. Geophys. Res., Vol. 86, N° Boll., 10515-10529.
- JAEGER J.C. (1957) - *The temperature in the neighborhood of a cooling intrusive sheet*. Amer. J. Sci., 255, p. 306-318.
- JOHANNES W. (1985) - *The significance of experimental studies for the formation of migmatites*. In: Ashworth J.R. (Editor) Migmatites. Blackie, Glasgow, 36-85.
- JUREWICZ S.R., WATSON E.B. (1985) - *The distribution of partial melt in a granitic system: the application of liquid phase sintering theory*. Geochim. Cosmochim.

- Acta, 49, 1109-1121.
- KILINC I.A., (1972) - *Experimental Study of Partial Melting of Crustal Rocks and Formation of Migmatites*. 24th IGC, Section 2, Montreal, 109-113.
- LE BRETON N., THOMPSON A.B. (1988) - *Fluid absent (dehydration) melting of biotite in metapelites in the early stages of crustal anatexis*. Contrib. Mineral. Petrol. (in press).
- LAMBERT I.B., ROBERTSON J.K., WYLLIE P.J. (1969) - *Melting Reactions in the System $KAlSi_3O_8$ - SiO_2 - H_2O to 18.5 kilobars*. Amer. J. Sci., Vol. 267, 609-626.
- LUTH W.C., (1969) - *The system $NaAlSi_3O_8$ - SiO_2 and $KAlSi_3O_8$ - SiO_2 to 20 kb and the relationship between H_2O content, P_{H_2O} and P_{total} in granitic magmas*. Amer. Jour. Sci., Schairer Vol. 267-A 325-341.
- LUTH W.C. (1976) - *Granitic rocks*. In: Bailey D.K., MacDonald R. (Editors), *The Evolution of the Crystalline Rocks*. Acad. Press, London.
- NANEY M.T. (1983) - *Phase equilibria of rock-forming ferromagnesian silicates in granitic systems*. Amer. J. Sci., 283, 993-1033.
- O'HARA M.J. (1976) - *Data reduction and projection schemes for complex compositions*. Progress in Exp. Petrol. NERC London, 3, 103-126.
- O'CONNOR J.T. (1965) - *A classification for quartz-rich igneous rocks based on feldspar ratios*. U.S.G.S. Prof. Paper 525-B, 79-84.
- PERCIVAL J.A. (1983) - *High-grade metamorphism in the Chapeau-Foley Area, Ontario*. Amer. Mineral., Vol. 68, 667-686.
- PETÖ P. (1976) - *An experimental investigation of melting relations involving muscovite and paragonite in the silica-saturated portion of the system K_2O - Na_2O - SiO_2 - H_2O to 15 kb total pressure*. Progress in Exp. Petrol. NERC London, 3, 41-45.
- PETÖ P., THOMPSON A.B. (1974) - *Wet and dry melting of white mica-alkali feldspar assemblages*. Trans. Am. Geophys. Un 55, 479.
- PIWINSKII A.J. (1975) - *Experimental studies of granitoid rocks near the San Andreas Fault Zone in the coast and transverse ranges and Mojave Desert, California*. Tectonophysics, 25, 217-231.
- RICHARDSON S.W., GILBERT M.C. BELL P.M. (1969) - *Experimental determination of kyanite-andalusite and andalusite-sillimanite equilibria; The aluminum silicate triple point*. Amer. J. Sci. 267, 259-272.
- RIDLEY J. (1986) - *Modelling of the relations between reaction enthalpy and the buffering of reaction progress in metamorphism*. Mineral. Mag. 50, 375-384.
- RUSHMER T. (1987) - *Fluid-absent melting of amphibolite-experimental results at 8 kbar*. Terra Cognita, 7, 286 (abs.).
- SHAW H.R. (19747) - *Diffusion of H_2O in granitic liquids*. pp. 139-169., In *Geochemical Transport and Kinetics* (eds. A.W. Hofmann et al.) Carnegie Inst. Washington Publ. 643.
- SHAW H.R. (1965) - *Comments on viscosity, crystal settling and convection in granitic systems*. Amer. J. Sci. 272, 120-152.
- STORRE B. (1972) - *Dry Melting of Muscovite + Quartz in the range $P_S = 7 kb$ to $P_S = 20 kb$* . Short Communications. Contr. Mineral. Petrol. 37, 87-89.
- THOMPSON A.B. (1982) - *Dehydration melting of pelitic rocks and the generation of H_2O -undersaturated granitic liquids*. Amer. J. Sci., 282, 1567-1595.
- THOMPSON A.B., ALGOR J.R. (1977) - *Model systems for anatexis of pelitic rocks. I. Theory of melting reactions in the system $KAlO_2$ - $NaAlO_2$ - Al_2O_3 - SiO_2 - H_2O* . Contrib. Mineral. Petrol. 63, 247-269.
- THOMPSON A.B., TRACY R.J. (1979) - *Model System for Anatexis of Pelitic Rocks. II. Facies Series Melting and Reactions in the System CaO - $KAlO_2$ - $NaAlO_2$ - Al_2O_3 - SiO_2 - H_2O* . Contrib. Mineral. Petrol. 70, 429-438.
- THOMPSON J.B. (1981) - *Composition space: An algebraic and geometric approach*. Reviews in Mineralogy, 10, 1-32.
- TUTTLE O.F., BOWEN N.L. (1958) - *Origin of granite in the light of experimental studies in the system $NaAlSi_3O_8$ - $KAlSi_3O_8$ - SiO_2 - H_2O* . Geol. Soc. Am. Mem. 74: 153 pp.
- WICKHAM S.M. (1987) - *The segregation of granitic magmas - some examples from the Pyrenees*. J. Geol. Soc. London (in press).
- WINKLER H.G.F. (1979) - *Petrogenesis of metamorphic rocks*. Springer-Verlag, New York.
- WYLLIE P.J. (1977) - *Crustal Anatexis: An experimental review*. Tectonophysics 43, 41-71.
- VIELZEUF O., HOLLOWAY J.R. (1988) *Experimental determination of the fluid-absent melting relations in the pelitic system. Consequences for crystal differentiation*. Contrib. Mineral. Petrol. 98, 257-276.
- VAN DER MOLEN I., PETERSON M.S. - (1979) - *Experimental deformation of partially-melted granite*. Contrib. Mineral. Petrol. 70: 218-229.